MATEC Web of Conferences **14**, 18003 (2014)
DOI: 10.1051/matecconf/20141418003

High-temperature γ (FCC)/γ' ($L1_2$) Co-Al-W based superalloys

Matthias Knop[1], Vassili A Vorontsov[1], Mark C Hardy[2], and David Dye[1,a]

[1] Department of Materials, Imperial College, Prince Consort Road, London SW7 2AZ, UK
[2] Rolls-Royce plc, PO Box 31, Moor Lane, Derby DE24 8BJ, UK

Abstract. Interim results from the development of a polycrystalline Co-Al-W based superalloy are presented. Cr has been added to provide oxidation resistance and Ni has then been added to widen and stabilise the γ' phase field. The alloy presented has a solvus of 1010 °C and a density of 8.7 g cm^{-3}. The room temperature flow stress is over 1000 MPa and this reduces dramatically above 800 °C. The flow stress anomaly is observed. A microstructure with both ∼ 50 nm γ' produced on cooling and larger 100–200 nm γ' can be obtained. Isothermal oxidation at 800 °C in air for 200 h gave a mass gain of 0.96 mg cm^{-2}. After hot deformation in the 650–850 °C temperature range, both anti phase boundaries (APBs) and stacking faults could be observed. An APB energy of 71 mJ m^{-2} was measured, which is comparable to that found in commercial nickel superalloys.

1. Introduction

Improved temperature capability alloys for the hot section of gas turbine engines are required to enable achievements in fuel economy and overall performance. Presently, Ni-base superalloys are used due to their high temperature strength and their environmental resistance. These alloys have a two phase γ/γ' microstructure which remains stable at temperatures near the melting point. In 2006, Sato *et al.* [1] discovered a phase in Co-base alloys which is similar to the γ' phase in Ni-base alloys, Ni_3Al. The stoichiometric composition of the newly discovered phase is $Co_3(Al,W)$. Additional work by Ishida *et al.* and Pollock *et al.* [2,3] has shown that alloys of this class can be improved with similar elemental additions to Ni-base superalloys. They also exhibit the characteristic flow stress anomaly and may be stronger at high temperatures.

In this paper, we present a candidate wrought Co-base superalloy that is being evaluated for potential future use in gas turbine engines. The γ' solvus temperature and density are provided, and the influence of the γ' microstructure on the flow stress over a wide temperature range is examined. Additionally, the oxidation behaviour under isothermal and cyclic conditions is presented.

2. Experimental procedures

The polycrystalline alloy presented in this paper was produced by ATI metals (*Pittsburgh, USA*). Its composition is within the range of a patent by the authors [4] and contains Co, Ni, W, Ta, 12 at.% of Cr and 10 at.% of Al. Ternary Co-Al-W alloys exhibit poor oxidation behaviour which can be improved by the addition of Cr. However, Cr destabilises the γ' phase [5]. To counteract this effect, Ni is added which expands the γ' phase field in this alloy class [6]. Ta additions are known to increase γ' solvus temperature and the high temperature strength [2].

Grain boundary strengtheners, Zr, B, C, were added to the alloy to increase its strength at elevated temperatures. These elements are known to be beneficial in Ni-base alloys [7].

The material was super-solvus forged at 1050 °C and furnace cooled with a subsequent ageing heat treatment of 16 h at 900 °C and furnace cool. This state will be referred to as the as-received condition.

Differential scanning calorimetry (*DSC*) was used to determine the γ' solvus temperature. A cuboidal sample with an edge length of 3 mm was placed in a alumina crucible and the tests were performed in an argon atmosphere. The sample was heated up to 1200 °C with a heating and cooling rate of 10 °C min^{-1}.

Scanning electron microscopy (*SEM*) was performed on a Zeiss Auriga FEGSEM with an accelerating voltage of 5 kV and a working distance of 5 mm. Secondary electron imaging was used to examine the γ/γ' microstructure. These samples were ground, polished and etched electrolytically using a potential of 2.5 V in a solution of 2.5% phosphoric acid in methanol. Samples from the oxidation tests were cut while mounted in epoxy to avoid spallation of the oxide scale. They were subsequently ground, polished and gold-coated prior to back-scattered electron imaging.

Compression tests were performed on cylindrical samples with a diameter of 6 mm and a height of 8 mm, coated with Acheson's Deltaglaze 3418 (except the room temperature sample) and tested at temperatures up to 900 °C. They were heated by an infra-red furnace with a heating rate of 100 °C min^{-1} while being held at a compressive pre-load of 100 N. Before the tests were started, a 3 min dwell time was used to ensure a uniform temperature distribution within the sample. These were

[a] Corresponding author: ddye@ic.ac.uk

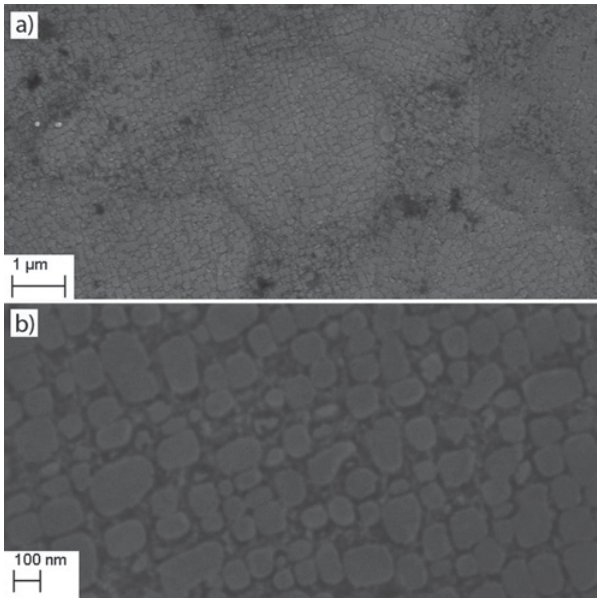

Figure 1. *SEM* micrographs (etched SEI), illustrating the γ/γ' microstructure of the alloy in the as-received condition.

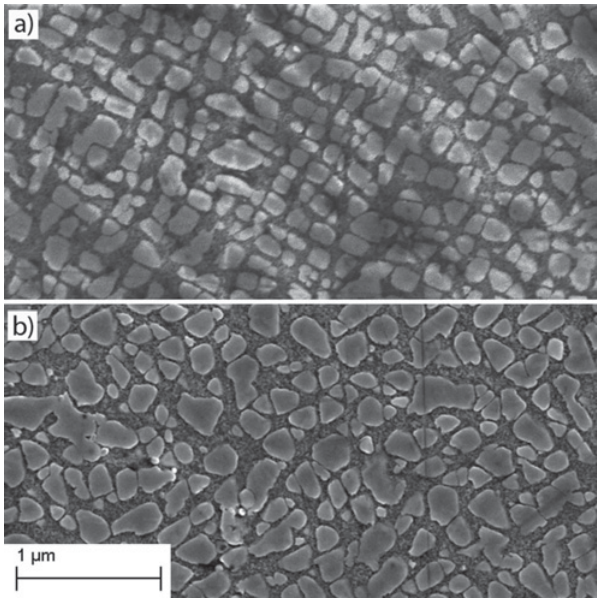

Figure 2. *SEM* micrograph (etched SEI), γ/γ' microstructure after (a) 1000 h and (b) 2000 h at 800 °C.

compressed, under true strain rate control, at a rate of $10^{-3}\,s^{-1}$.

The compression samples were analysed using an FEI Titan 80-300 transmission electron microscope. 300 μm thick slices were cut perpendicular to the load axis. 3 mm diameter discs were then spark eroded and subsequently twin-jet electropolished at a bias potential of 25 V at −30 °C in a solution of 5% perchloric acid in methanol.

Oxidation experiments were conducted at 800 °C. The samples for the isothermal and cyclic oxidation experiments were 20 mm × 10 mm × 2 mm in size and surface ground with 800 grit SiC paper. For isothermal oxidation, the samples were placed in a furnace in alumina crucibles and exposed to laboratory air. After 200 h the samples were taken out of the furnace, remaining in the crucibles to contain any spalled oxide during air cooling. They were weighed before and after exposure to determine their mass change. The cyclic oxidation tests were performed using an automatic stage which inserted and extracted the samples into and from a tube furnace. The samples remained in the furnace for 48 min in laboratory air and out of the furnace for 12 min to cool down and allow time for the weighing process. They were tested for 200 cycles.

3. Results

The SEM micrographs in Fig. 1 show the microstructure of the alloy in the as-received condition. The secondary γ' precipitates were 100 to 200 nm in size and the tertiary precipitates were less than 20 nm in size. No other phases were observed in the alloy.

It has been shown that γ' is metastable in ternary Co-Al-W alloys [8] and therefore long term stability heat treatments were conducted. The samples remained at 800 °C for 1000 h (Fig. 2a) and 2000 h (Fig. 2b), respectively. The coarsening of the γ' precipitates was found to be relatively slow and formation of other phases was not observed.

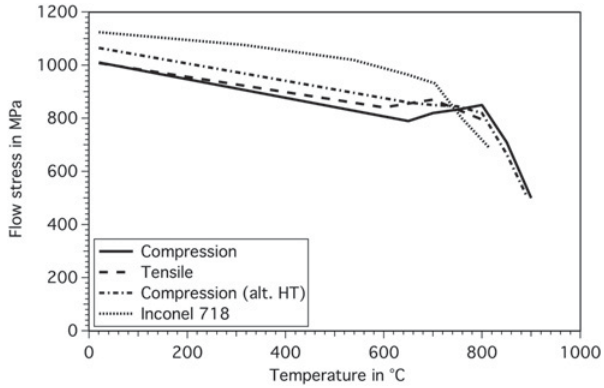

Figure 3. Flow stress behaviour with temperature for compression and tensile tests of the as-received alloy, compression tests of the alternative heat treatment, showing fully heat treated tensile data for Inconel 718 as comparison.

The γ' solvus temperature of the presented alloy was determined from the *DSC* data to be 1010 °C. Its density was measured to be $8.7\,g\,cm^{-3}$.

Figure 3 shows the results of the compression tests conducted on this alloy. The solid line represents the as-received samples. It exhibits the anomalous behaviour known from Ni-base alloys, where the flow stress increases with increasing temperature, in this case at 650–800 °C. At room temperature the flow stress is above 1000 MPa which deceases until 650 °C, increases up to 800 °C to 850 MPa, followed by a rapid decrease beyond that.

Additionally, tensile tests were performed at Exova Plzen at various temperatures. The results, which are in good agreement with the compression data, are also shown in Fig. 3.

The γ/γ' microstructure of the alloy in the as-received condition is not optimised. To study the influence of

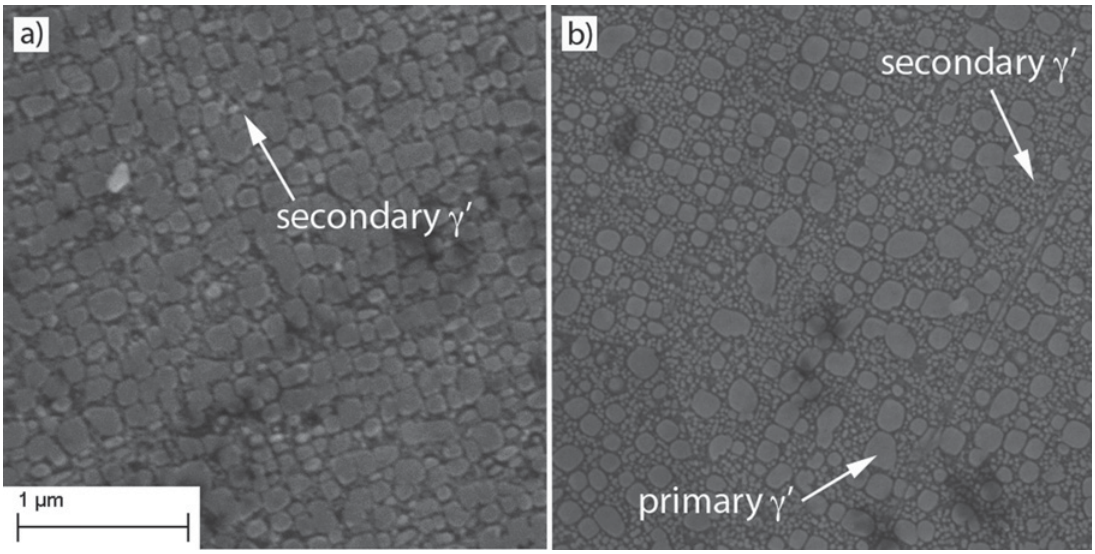

Figure 4. *SEM* micrograph (etched, SEI), γ/γ' microstructure, as-received (a) and alternative heat treatment (b) – homogenised at 980 °C for 1 h, water-quenched, aged at 830 °C for 2 h, air-cooled).

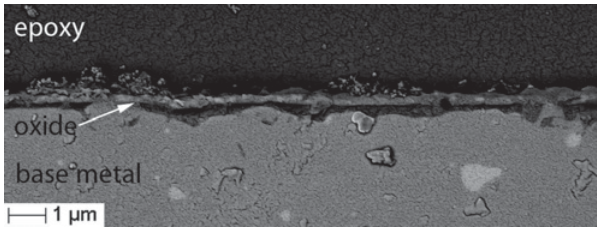

Figure 5. Cross-sectional view of the oxide scale above the base alloy after 200 h isothermal oxidation at 800 °C (sample is gold-coated, BSE mode).

this microstructure on the flow stress a different heat treatment was conducted, similar to [9]. The as-received samples were homogenised at 980 °C for 1 h with a subsequent water-quench. This dissolves most of the secondary and all of the tertiary γ'. Thus, the remaining secondary γ' are then termed primary precipitates. After the homogenisation, the samples were aged at 830 °C for 2 h. During this step the secondary γ' precipitates coarsened, with a high number density of γ' precipitates $\sim$ 50 nm in diameter being observed (Fig. 4b). The results of this test series are shown in Fig. 3. The flow stress up to 750 °C is higher for the samples with the alternative heat treatment but slightly lower beyond 750 °C.

As a comparison, tensile data for the Ni-base alloy Inconel 718 are shown in Fig. 3. This alloy also exhibits a high strength at lower temperatures up to 700 °C but its strength rapidly decreases above that temperature.

A cross-section of the oxide scale of a sample after isothermal oxidation for 200 h at 800 °C is shown in Fig. 5 and the mass change is given in Table 1. For comparison, values for a typical Ni-base superalloy, a modified Udimet 720, (calculated from k_p value) and a solid-solution hardened Co-base alloy Haynes 188 are also given [10,11]. The continuous and adherent oxide scale observed was between 0.5 and 1 μm thick. Spallation of the oxide was not observed. Formation of other phases,

Table 1. Average mass change of the alloy after isothermal oxidation (200 h at 800 °C). Mass gain of Udimet 720 [10] (calculated) and Haynes 188 [11] are given for comparison.

Alloy	**Cr-content**	**Areal mass gain**
	at.%	*mg cm*$^{-2}$
Presented alloy	12	0.96
Udimet 720	19	0.43
Haynes 188	26	0.17

Table 2. Average mass change of the alloy after isothermal oxidation (200 h at 800 °C) and cyclic oxidation (200 cycles, each composed of 48 min at 800 °C and 12 min out of the furnace cooling towards room temperature).

Type	**Time at 800 °C**	**Areal mass gain**
	h	*mg cm*$^{-2}$
Isothermal	200	0.96
Cyclic	167	0.77

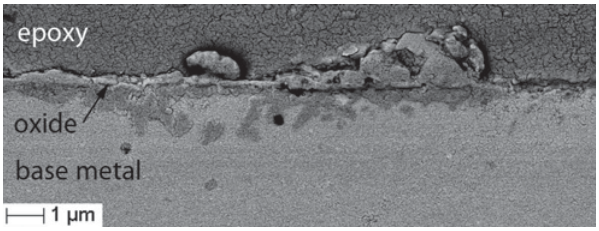

Figure 6. Cross-section of the oxide scale after 200 cycles (48 min in the furnace, 12 min out of the furnace) at 800 °C (sample gold-coated, BSE mode).

such as Co_3W, was not observed in the base metal beneath the oxide.

The results of the cyclic oxidation tests are given in Table 2. The mass gains during these experiments were similar to those in the isothermal tests. The lower value

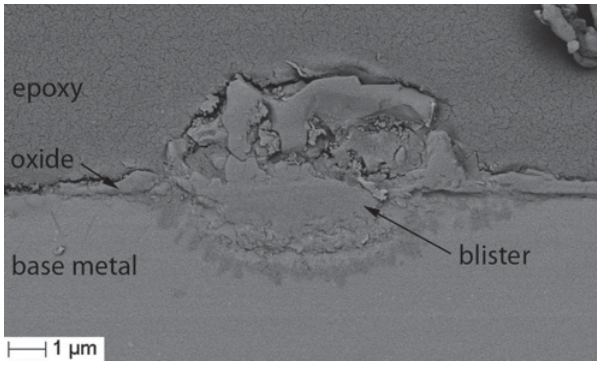

Figure 7. Oxide feature observed after cyclic oxidation. Cross-section of the oxide scale after 200 cycles (48 min in the furnace, 12 min out of the furnace) at 800 °C, sample gold-coated, BSE mode).

directly correlates to the shorter time at 800 °C. Figure 6 shows a cross-section of the oxide scale after the cyclic tests. The scale is not as uniform as that found in the isothermal oxidation samples and more internal oxide formation was observed. The thickness of the scale varied between 1 and 4 μm. In addition, some regions show the formation of blister-like features (Fig. 7) which has a thicker outer oxide scale and more severe internal oxidation. Overall, the results obtained are encouraging relative to the value of 3 mg cm^{-2} obtained for Co-9Al-9W-0.12B (at.%) [12].

4. Discussion

As shown above, the γ/γ' microstructure is stable for at least 2000 h at 800 °C in these alloys. Ishida reported in [6] that the γ' phase field is continuous from Co-Al-W to Ni-Al-W alloys. This increases the phase field and therefore stability of γ' when Ni is added to Co-Al-W alloys. Also, the γ' phase field shifts towards higher Al and lower W contents with increasing Ni content in these alloys and therefore reduces their density. Studies performed previously by the authors suggest that the limits of Cr and Al additions while maintaining a γ/γ' microstructure are 15 at.% and 10 at.%, respectively.

The compression tests were interrupted after only a few per cent plastic strain in order to allow for the dislocation structures to be examined by transmission electron microscopy. A foil removed from a sample deformed at 750 °C showed extensive dislocation activity in the γ channels, and what appeared to be an anti phase boundary (APB) pair in the γ', Fig. 8a. This suggests that the matrix strength should be increased in future alloy developments. The measured spacing d was found to be 4.1 nm. Correcting this for the 10° tilt from the {111} gives an APB spacing of 4.2 nm. Using a shear modulus G of 101 Gpa [13,14], which is agreed upon by both experiment and theory, and a γ' lattice parameter of $a =$ 3.68 Å measured in the TEM, allows the APB energy to be calculated. The APB energy γ_{APB} is given by

$$\gamma_{\mathrm{APB}} = K\frac{Gb^2}{2\pi d} \qquad (1)$$

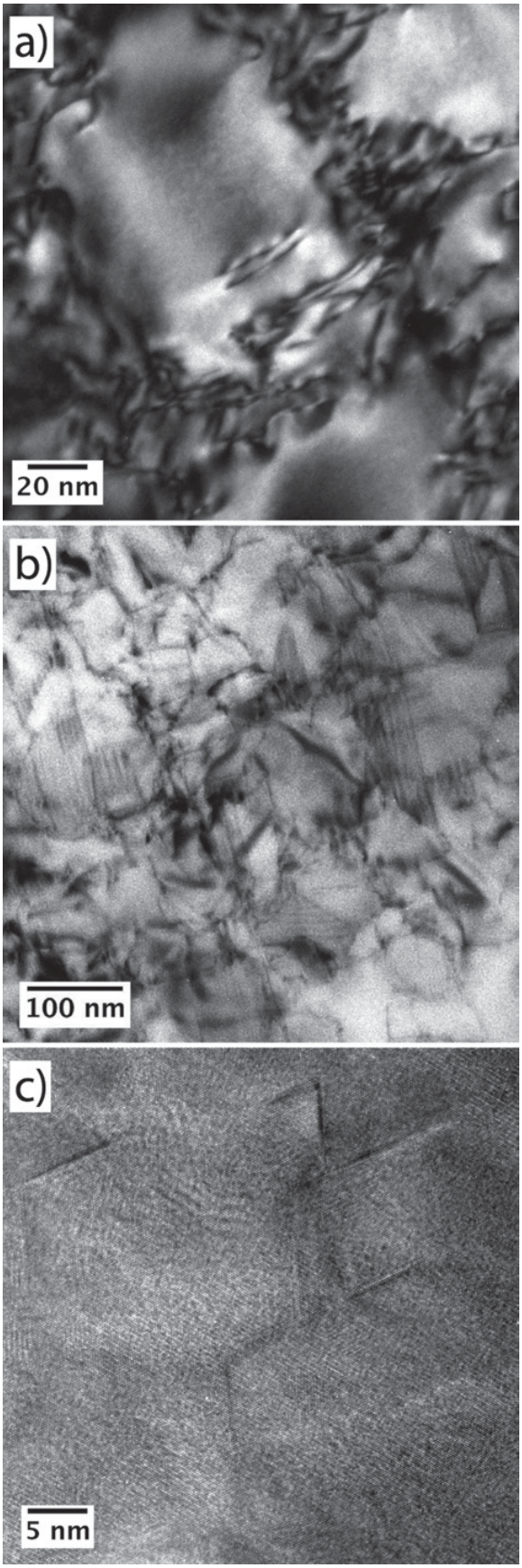

Figure 8. (a) and (b) BF TEM and (c) HRTEM images of the dislocation structures found after deformation at 750 °C (a) and 850 °C (b), (c).

where K is a constant equal to 1 for screw dislocations and b is the Burgers vector [15]. Therefore, the measured APB energy is 71 mJ m^{-2}.

For comparison, the {111} APB energy of $Co_3(Al,W)$ has been found to be 146 mJ m^{-2} [16], and in pure Ni_3Al, 180 mJ m^{-2} [17]. In both systems, Ti and Ta are suspected to substantially raise the APB energy [17,18], but values of as low as 118 mJ m^{-2} are found in commercial superalloys, presumably because other alloying elements such as Cr decrease the APB energy. Recent atomistic calculations suggest that in Co-Ni alloys, the SFE may be lower than in either alone, which is consistent with the comparatively low APB energy found here.

The APB energy is of course important as it provides a contribution to the precipitation hardening provided by the γ', together with the coherency strain due to the lattice misfit. High fault energies are particularly desirable as, while misfit promotes coarsening through the concomitant surface energy, fault energies affect only strength. Even for deformation mechanisms associated with stacking fault shear, the $a\langle 112\rangle$ superdislocation ribbon will have an APB at its core between the partial dislocations, and so the APB energy remains of interest.

Stacking faults could also be observed in the γ', Fig. 8b. These were commonly found in foils extracted from samples below (650 °C), at (750 °C) and above (850 °C) the flow stress anomaly. These were also observed using high resolution imaging, Fig. 8c. Here the stacking fault segments could be observed to terminate each other, implying that they are either cross-slipped and locked, or that different stacking faults that have interacted with each other, providing forest hardening. Characterisation and understanding of the stacking fault mechanisms remains the subject of further work.

To evaluate the influence of the γ/γ' microstructure on the mechanical properties, an alternative heat treatment was performed on the alloy. The difference between the as-received and the alternative heat treatment samples was the amount of the primary/secondary γ' as well as the amount and size of the tertiary/secondary γ' precipitates. The finer secondary γ' after the alternative heat treatment improved the flow stress at lower temperature because their size (∼50 nm) is in the range that provides maximum resistance to cutting by weakly coupled dislocation pairs. This leads to cutting by strongly coupled pairs [9]. On the other hand, the fine tertiary/secondary γ' start to dissolve at temperatures above 750 °C and their strengthening effect disappears. The as-received alloy is stronger at these higher temperatures because of the higher volume fraction of γ' precipitates between 100 and 200 nm in size.

In addition to the mechanical properties the oxidation behaviour is also important for the performance of the alloy. The oxide scale after the isothermal oxidation is adhered, relatively even and continuous. This suggests that a protective layer of oxide is formed early in the process which prevents further oxidation of the samples.

Most Co-Al-W alloys in the literature form Co_3W underneath the oxide scale [12]. Their Al_2O_3 layer depletes the underlying base metal of Al, thereby enriching it in W. This favours formation of Co_3W instead of γ'. The absence of Co_3W in the presented alloy suggests that the zone underneath the oxide scale is not depleted sufficiently in Al to destabilise γ'. This can be explained by the higher Al and lower W contents.

The Co-base alloy, Haynes 188, used for comparison is a solid-solution and carbide strengthened alloy containing 26 at.% Cr, whereas the classic disc alloy Udimet 720 studied by Chen contained 19 at.% Cr [10]. These higher Cr contents favour the formation of Cr_2O_3 scales earlier during oxidation and protect the alloy more effectively.

Similar mass gains of the samples after cyclic and isothermal oxidation may mean that the adhesion of the oxide scale is sufficient to avoid severe cracking or spallation. Although, the difference in appearance of the scale after cyclic oxidation could mean that it takes more time to form a protective oxide. This would explain the more pronounced internal oxide formation and the overall less even scale.

The oxide scale of the blister-like feature looks similar to scales of alloys with low Cr contents [5] which may be due to localised compositional fluctuations. In those cases, a relatively thick outer Co_3O_4 layer forms, underneath a complex mixed oxide and finally a protective Al_2O_3 layer [5]. The addition of 15 at.% instead of 12 at.% Cr might be sufficient to avoid these occurrences and promote the formation of a scale similar to that formed during isothermal conditions.

5. Conclusions

The findings in this study suggest that practical polycrystalline Co-base superalloys, strengthened by γ', may be possible;

- The alloys maintain a two phase γ/γ' microstructure with higher additions of Cr when stabilised by Ni,
- the density (8.7 g cm^{-3}) needs to be reduced, which can be achieved by adjusting the composition,
- the γ' solvus temperature (1010 °C) is high enough for the possible upper service temperature of 800 °C but may present additional manufacturing challenges,
- the oxidation behaviour is acceptable, but could be improved by alloying,
- the flow stresses found at room temperature (>1000 MPa) and up to 800 °C (>800 MPa) are satisfactory.

It is suggested that optimisation of the microstructure could improve the mechanical properties significantly.

The authors would like to acknowledge the financial support provided by Rolls-Royce plc, Imperial College London and EPSRC (UK) grant EP/H022309/1. Useful conversations with Hui-Yu Yan (Imperial) and Howard Stone (Cambridge) are also acknowledged.

References

[1] J. Sato, T. Omori, K. Oikawa, I. Ohnuma, R. Kainuma and K. Ishida. *Science*, **312** 90–91 (2006)
[2] A. Suzuki, G.C. DeWolf and T.M. Pollock. *Scripta Mater.*, **56** 385–388 (2007)

[3] A. Suzuki and T.M. Pollock. *Acta Mater.*, **56** 1288–1297 (2008)
[4] D. Dye, M. Knop, H.-Y. Yan, M.C. Hardy and H.J. Stone. GB patent GB1312000.1, NY, USA (2013)
[5] H.-Y. Yan, V.A. Vorontsov and D. Dye. *Intermet.*, **48** 44–53 (2014)
[6] K. Ishida. In *MRS Proceedings*, **1128-U06-06** (2008)
[7] R. Bürgel. *Handbuch Hochtemperatur-Werkstofftechnik*. Vieweg (2006)
[8] S. Kobayashi, Y. Tsukamoto, T. Takasugi, H. Chinen, T. Omori, K. Ishida and S. Zaefferer. *Intermet.*, **17** 085–1089 (2009)
[9] M.P. Jackson and R.C. Reed. *Mater. Sci. Eng. A*, **259** 85–97 (1999)
[10] J.H. Chen, P.M. Rogers and J.A. Little. *Oxid. Met.*, **47** 381–410 (1997)
[11] B.A. Pint. In *Shreir's Corrosion*, Vol. 1, 606–645. Elsevier B.V., 4th edition (2010)
[12] L. Klein, A. Bauer, S. Neumeier, M. Göken and S. Virtanen. *Corros. Sci.*, **53** 2027–2034 (2011)
[13] K. Tanaka, T. Ohashi, K. Kishida and H. Inui. *Appl. Phys. Let.*, **91** 181907 (2007)
[14] C. Jiang. *Scripta Mater.*, **59** 1075–1078 (2008)
[15] M.J. Marcinkowski, N. Brown and R.M. Fisher. *Acta Metal.*, **9** 129–137 (1961)
[16] N.L. Okamoto, T. Oohashi, H. Adachi, K. Kishida, H. Inui and P. Veyssieère. *Philos. Mag.*, **91:28** 3667–3684 (2011)
[17] F. Diologent and P. Caron. *Mater. Sci. Eng. A*, **385** 245–257 (2004)
[18] A. Mottura, A. Janotti and T.M. Pollock. *Intermet.*, **28** 138–143 (2012)